Current Research in Toxicology 6 (2024) 100154

Contents lists available at ScienceDirect

Current Research in Toxicology

journal homepage: www.journals.elsevier.com/current-research-in-toxicology

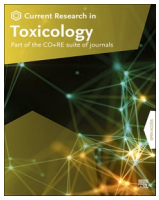

Perfluorooctanesulfonic acid (PFOS) disrupts cadherin-16 in the developing rat thyroid gland

Nichlas Davidsen, Louise Ramhøj, Anne-Sofie Ravn Ballegaard, Anna Kjerstine Rosenmai, Cecillie Sofie Henriksen, Terje Svingen *

National Food Institute, Technical University of Denmark, Kgs. Lyngby DK-2800, Denmark

ARTICLE INFO

Keywords:
PFAS
PFOS
Thyroid
Development
Ex vivo
Cadherin 16
Perfluorooctane sulfonate

ABSTRACT

Perfluorooctanesulfonic acid (PFOS) can disrupt the thyroid hormone (TH) system in rodents, potentially affecting perinatal growth and neurodevelopment. Some studies also suggest that gestational exposure to PFOS can lead to lower TH levels throughout life, indicating that PFOS may compromise thyroid gland development. To address this question, we utilized a rat thyroid gland *ex vivo* culture system to study direct effects of PFOS on the developing thyroid. No significant changes to follicular structure or size were observed with 1 μM or 10 μM PFOS exposure. However, the transcription factor *Foxe1*, together with *Tpo* and *Lrp2*, were upregulated, whereas the key transcription factor *Pax8* and its downstream target gene *Cdh16* were significantly downregulated at the transcript level, observed with both RT-qPCR and RNAscope. Notably, *Cdh16* expression was not uniformly downregulated across *Cdh16*-postive cells, but instead displayed a patchy expression pattern across the thyroid gland. This is a significant change in expression pattern compared to control thyroids where *Cdh16* is expressed relatively uniformly. The disrupted expression pattern was also seen at the protein level. This suggests that PFOS exposure can impact follicular growth and structure. Compromised follicle integrity, if irreversible, could help explain reduced TH synthesis postnatally. This view is supported by observed changes to *Tpo* and *Lrp2* expression, two factors that play a role in TH synthesis.

Introduction

The synthetic chemical perfluorooctanesulfonic acid (PFOS) can disrupt fetal development in both humans and animals (Fenton et al., 2021). Notably, PFOS can disrupt the thyroid hormone (TH) system of human infants (Aimuzi et al., 2019; Preston et al., 2020), rat pups (Yu et al., 2009b), and zebrafish larvae (Shi et al., 2008) and PFOS have been found in human thyroid tissue (Pirali et al., 2009). Several rodent studies suggest that perfluorinated compounds can interfere with the TH system during perinatal stages and cause lasting effects seen as compromised TH levels later in life. For example, rat pups prenatally exposed to PFOS show decreased total thyroxine (T4) and free T4 levels until postnatal day (PND) 35 (Lau et al., 2003; Yu et al., 2009b), an effect that persist even if the body burden of PFOS declines (Yu et al., 2009b). Similarly, gestational exposure to perfluorohexane sulfonate (PFHxS) can markedly reduce serum T4 in newborn rats (Gilbert et al., 2021), whereas exposure to perfluorobutane sulfonate (PFBS) can reduce both T3 and T4 in newborn mice, persisting until PND60 (Feng et al., 2017). Since the effects of early-life exposure persist into puberty and adulthood, it could suggest that at least some perfluorinated compounds can directly affect fetal thyroid gland development and cause irreversible damage manifesting as compromised capacity to synthesize THs.

Lifelong thyroid function depends on correct thyroid gland development, which is regulated by a network of transcription factors, including Haematopoietically-expressed homeobox (*Hhex*), NK2 homeobox 1 (*Nkx2-1*), Paired Box 8 (*Pax8*), and Forkhead box E1 (*Foxe1*) (López-Márquez et al., 2021; Nilsson and Fagman, 2017). These factors orchestrate early thyroid gland development and later folliculogenesis, and continue to be important for thyroid gland function throughout life (Damante et al., 2000; López-Márquez et al., 2021; Nilsson and Fagman, 2017; Parlato et al., 2004). Follicle formation, growth, and maintenance of basal–apical membrane integrity are key components of TH biosynthesis and release (Koumarianou et al., 2017). Here, PAX8 and its target gene *Cadherin-16* (*Cdh16*) establishes and maintains the apical-basal polarization needed for follicle formation, lumen expansion, and TH synthesis (Johansson et al., 2021; Koumarianou et al., 2017). After the

* Corresponding author.
E-mail address: tesv@food.dtu.dk (T. Svingen).

https://doi.org/10.1016/j.crtox.2024.100154
Received 23 November 2023; Received in revised form 1 February 2024; Accepted 5 February 2024
Available online 6 February 2024

onset of thyroid function, which occur around gestation day (GD) 19 (embryonic day 18) in rats (De Escobar et al., 2004), *Nkx2-1*, *Pax8*, and *Foxe1*, together with thyroid stimulating hormone (TSH) partly controls the expression of key factors in TH synthesis, including thyroglobulin (TG), thyroperoxidase (TPO) and the sodium-iodide symporter (NIS) (Maenhaut et al., 1992; Postiglione et al., 2002).

Although PFOS is known to disrupt the TH system, knowledge about how disruption may occur at the tissue and molecular level is limited. Regarding thyroid gland development, gestational exposure to PFOS was shown to increase around 2-fold the number of proliferating thyroid epithelial cells in female rat fetuses (Chang et al., 2008). In non-mammalians, a mixture of PFAS could reduce relative colloid area and thyroid follicular size, together with a decline in free T4 and T3 in chicken embryos (Mattsson et al., 2019), whereas PFOS could lower the expression of *Hhex* and *Pax8* in zebrafish larvae (Shi et al., 2008). Additional information could potentially be obtained from studies in adult rodents where PFOS exposure significantly reduces circulating levels of T4 and T3 (Curran et al., 2008; Davidsen et al., 2022; Thibodeaux et al., 2003; Yu et al., 2009a). However, the thyroid gland transcriptome does not seem to be strongly affected by PFOS in adult rats (Davidsen et al., 2022).

Other suggested mechanisms by which PFOS can interfere with the TH system includes inhibition of the sodium-iodide symporter (NIS) (Buckalew et al., 2020; Conti et al., 2020; Wang et al., 2019, 2018), antagonism of the thyroid receptor (TR) alpha (Ren et al., 2014), displacement of T4 from the TH distributor protein transthyretin (TTR), and disruption to TH metabolism and excretion in the liver (Chang et al., 2008; Ren et al., 2016; Weiss et al., 2009; Yu et al., 2011, 2009b). These mechanisms could play a role in the continued thyroid hormone system disruption by PFOS but since the developmental effects are persistent, other mechanisms could also contribute to, or be responsible for, the persistent effects on TH levels following developmental exposure. To start addressing the issue, a first step would be to look more closely at the developing thyroid gland under PFOS exposure. Hence, we designed a study using explanted rat thyroid glands to assess if PFOS could directly affect fetal thyroid development, focusing on key transcription factors and their downstream targets, in addition to indices of TH synthesis.

Materials and methods

Ex vivo culture

Seven time-mated, nulliparous Sprague-Dawley rat dams (Crl:CD (SD) bred by Charles River Europe, and distributed by SCANBUR, (Karlslunde, Denmark) arrived on gestation day (GD) 17 (the day of plug-detection designated GD1). On GD21, dams were decapitated under CO_2/O_2 anaesthesia, and the fetuses collected and immediately killed by decapitation. The animal experiments were carried out in the BioFacility of the Technical University of Denmark. Ethical approval was given by the Danish Animal Experiments Inspectorate, authorization number 2020–15-0201–00539. The experiments were overseen by the in-house Animal Welfare Committee for animal care and use at the National Food Institute. Housing conditions and animal care were as detailed in Ramhøj et al. (2022).

Thyroid glands were excised under stereomicroscope from GD21 male rat fetuses and stored (<2 hrs) in DMEM/F12 (Sigma-Aldrich, St. Louis, MO, USA). Both lobes from each thyroid gland were cultured together in hanging drop culture throughout the experiment. The culture was maintained using StemPro34 medium, with added StemPro34 nutritional supplement (Gibco, MA, USA), 0.25 U/mL penicillin–streptomycin (#15070063, Gibco), and 2 mM L-glutamine (#25030149, Gibco). Exposure conditions were 0 (DMSO control), 1 μM PFOS, 10 μM PFOS or 100 μM PFOS (Perfluorooctanesulfonic acid/Heptadecafluorooctanesulfonic acid potassium salt (PFOS) (CAS: 279–39-3, purity: 98 %, Sigma-Aldrich). The exposure concentrations were selected based on available literature evaluating thyroid effects *in vitro* (Buckalew et al., 2020; Conti et al., 2020; Coperchini et al., 2014). All samples were exposed to a basal level of 1 μM bovine thyroid stimulating hormone (TSH) (#TSH-1315B, Creative Biomart, NY, USA) and 0.1 % dimethyl sulfoxide (DMSO) (CAS: 67–68-5, Sigma-Aldrich) in the medium. The hanging drop culture was setup by pipetting 50 μL droplets of exposure medium on the inner sides of reversed lids of 24-well Cellstar plates (Greiner, Austria). One thyroid gland was placed in each droplet and the lids flipped in one swift motion and mounted on the 24-well plates. Thus, the droplets containing the thyroid glands, were hanging from the lid, each drop above one well filled with PBS to reduce evaporation. Exposure medium (including chemicals, TSH and DMSO) was changed after 24hrs by flipping the lids, aspiring the old medium droplet and adding fresh exposure medium. The thyroid glands were cultured for a total of 48 hrs in an incubator at 37 °C, 80 % O_2, 5 % CO_2, 80 % relative humidity. The concentration of 100 μM PFOS proved too high for the hanging drop culture setup, with the drops unable to support the tissue. We therefore excluded the 100 μM exposure group from the study. After 48 hrs of culture the thyroid glands were collected and either stored at −80 °C for RNA extraction or stained with Meyer's haematoxylin and fixed in 10 % neutral buffered formalin (2 hrs) then transferred to 70 % EtOH (<4 days). The thyroid glands were processed, embedded in paraffin- and sectioned serially at 4 μm. Two sections (from two different tissue-depths) per thyroid lobe were evaluated.

Gene expression analysis

Total RNA was isolated from thyroid glands using Qiagen RNeasy micro kit (Qiagen, Hilden, Germany) with on-column DNase I treatment. Quantity and purity of RNA was measured using a NanoDrop spectrophotometer (ND-1000, Fisher Scientific), with a 260/280 ratio threshold ≥ 1.90. 500 ng RNA was used for cDNA synthesis using the Omniscript Reverse Transcription Kit (Qiagen) together with anti-RNAse and Random primer mix from Invitrogen (MA, USA). TaqMan Gene Expression assays (Life Technologies, Carlsbad, CA, USA) were used as follows: transcripts related to thyroid gland function; *Tshr* (Rn00563612_m1), *Slc5a5* (Rn00583900_m1), *Duox1* (Rn00596688_m1) *Tpo* (Rn00571159_m1), *Tg* (Rn00667257_g1), *Lrp2* (Rn00578067_m1), *Dio1* (Rn00572183_m1). Thyroid gland development and specification; *Nkx2-1* (Rn01512482_m1), *Pax8* (Rn00579743_m1), *Foxe1* (Rn00594363_s1), *Cdh16* (Rn01536488_m1), *Cdh1* (Rn00580109_m1), *Cldn1* (Rn00581740_m1). Other probes selected were; *Nectin1* (Rn01421928_m1), *Pclaf* (Rn01644485_g1), *Kcnip3* (Rn00583484_m1), *Wnt5b* (Rn01492357_m1), and *Asgr1* (Rn00560750_m1). RT-qPCR was run in technical duplicates on a Quantstudio 7 Flex Real-Time PCR System (Applied Biosystems, Waltham, MA, USA), using 3 μL diluted (1:20) cDNA in each 11 μL reaction with TaqMan Fast Universal Mastermix (Life Technologies). The geometric mean of the stably expressed reference genes *Rps18* (Rn01428913_gH), and *SDHA* (Rn00590475_m1) was used to calculate relative transcription levels with the $2^{-\Delta\Delta Ct}$ method (Schmittgen and Livak, 2008).

In situ hybridization with RNAscope

Spatial gene expression was evaluated by RNAscope (Advanced Cell Diagnostics Biotechne, Newark, CA, USA) *in situ* hybridization in thyroid glands exposed to control and 10 μM PFOS (n = 4). The sections were deparaffinized and stained using the RNAscope® 2.5 HD - RED assay (Advanced Cell Diagnostics Biotechne) according to the manufacturer's instructions with 15 min RNAscope H202 and Protease Plus (Advanced Cell Diagnostics Biotechne) treatment, RNAscope Wash Buffer Reagents (Advanced Cell Diagnostics Biotechne) and reagents provided with the kit (Wang et al., 2012). The following RNAscope® target probes were used; *Foxe1* (Rn-Foxe1-C1), *Pax8* (Rn-Pax8-C1), *Cdh16* (Rn-Cdh16-C1). *Ppib* (Rn-Ppib) with and without xylene was used as positive control.

Sections were counterstained with Meyer's haematoxylin. The slides were scanned using a 40x objective in a Pannoramic Midi II digital slide scanner (3DHISTECH Ltd., Budapest, Hungary). Images were qualitatively evaluated with the SlideViewer 2.5 software (3DHISTECH Ltd.).

Immunohistochemistry (IHC)

IHC staining was conducted to evaluate expression of CDH16, LRP2, and PCLAF using two sections per thyroid gland. Staining was performed with slides mounted in Shandon Sequenza Immunostaining racks (Thermo Scientific, Denmark). The slides were dried and pre-heated at 60 °C. Sections were de-paraffinized, boiled in a microwave for 15 min in Tris/EDTA buffer with pH 9 and blocked with 1 % bovine serum albumin (BSA) in PBS for 30 min. The antibodies were diluted in 1 % BSA PBS buffer using ratios 1:8000 for CDH16 (ab212243, Abcam, UK), 1:25 for PCLAF (sc-390515, Santa Cruz Biotechnology Inc., TX, USA), and 1:100 for LRP2 (sc-515750, Santa Cruz Biotechnology Inc.). Slides were incubated with antibody for 30 min at RT. Blocking of endogenous peroxidase was conducted with 3 % H_2O_2 for 10 min at RT before incubation with EnVision + for 30 min. Successively, the sections were incubated for 15 min with DAB + and counter-stained with Meyer's haematoxylin. The slides were scanned using a 40x objective in a Pannoramic Midi II digital slide scanner (3DHISTECH Ltd.). SlideViewer 2.5 (3Dhistech Ltd., Hungary) was used to export the images for evaluation in Fiji.

Quantification of antibody staining and follicle formation

Fiji software was used to quantify the area of LRP2- and PCLAF-positive staining, number of follicles, and follicle diameter (Schindelin et al., 2012). For LRP2 and PCLAF quantification, images were converted to 8-bit format, then background removed using the inbuilt threshold function in Fiji. For one section per sample the mean area of antibody-positive staining relative to the assessed area was calculated using three randomly placed 400x400 pixel squares. The mean % area for each exposure group was calculated based on sample means. The threshold for background removal was the same for all sections.

The number of follicles (with lumen) was manually counted on the LRP2 stained sections. Follicles were counted within the three 400x400 pixel square used in the LRP2 quantification, averaged across the three squares, and expressed as number of follicles per mm^2 tissue. Follicle size was determined by measuring the diameter of 7–10 follicles, with an identifiable lumen, per thyroid lobe, using the measure function in the Fiji software scaled to the scale bar of each image (Schindelin et al., 2012).

Statistical analysis

Follicle number and size data (n = 4) are presented as mean ± standard deviation (SD) with individual data points shown as circles, the data was checked for normality using qqplot and significant effects were calculated using unpaired *t* test. Gene expression (n = 5–6) and IHC data (n = 4) are presented as mean ± standard deviation with individual datapoints shown as circles. Data were checked for normality using qqplot and Bartlett's test for variance. One-way ANOVA followed by post hoc Dunnett's test was conducted when assumptions were met. If assumptions for ANOVA were not met, Kruskal-Wallis followed by post hoc Dunn's test was conducted. The statistical significance level was set at $p < 0.05$ and is presented with *.

Results

PFOS exposure did not significantly affect thyroid morphology

Fetal rat thyroid glands were cultured *ex vivo* to determine if PFOS could directly affect the developing gland. At the morphological level PFOS exposure caused no signs of overt toxicity nor a significant effect on the number of follicles or follicle size, albeit a tendency towards increasing number and diameter were observed in PFOS-exposed thyroids (Fig. 1).

PFOS exposure disrupted expression of key genes involved in thyroid gland development and function

PFOS exposure affected transcript levels of the transcription factors *Pax8* and *Foxe1* (Fig. 2). *Foxe1* was significantly and dose-dependently upregulated in the 10 μM PFOS group (Fig. 2B). *Pax8* was significantly downregulated by 1 μM and 10 μM PFOS (Fig. 2C). We also visualized the expression of *Foxe1* and *Pax8* by RNAscope. Here, the expression was very strong and uniform across the tissue. No clear difference could be distinguished between controls and 10 μM PFOS (data not shown). There were no effects on *Nkx2-1* expression by RT-qPCR analysis (Fig. 2A).

Since PFOS disrupted expression of the key network of transcription factors in the developing thyroid gland, we proceeded to evaluate potential downstream effects on genes regulated by the same transcription factors. PFOS reduced the expression of *Cdh16* at 1 μM and 10 μM (Fig. 3A). Neither *Cdh1* nor *Cldn1* were significantly affected by PFOS exposure (Fig. 3B and 3C).

PFOS exposure decreased the number of CDH16-positive cells in the developing thyroid gland

To further characterize the effect on *Cdh16* within the thyroid gland, we performed RNAscope analyses to evaluate potential spatial expression changes. In the exposed thyroids, *Cdh16* exhibited patchy expression pattern in response to 10 μM PFOS (Fig. 4). Notably, this downregulation was not uniform across the thyroid gland, but instead appeared to be reduced, and even absent, in regions of the glands, with other regions still expressing high levels of mRNA. In the control thyroid glands, *Cdh16* expression was relatively uniform across the entire section with some areas of very high abundance.

Using an antibody against CDH16, we next analysed if the same disrupted expression pattern was occurring at the protein level. IHC staining confirmed the patchy expression pattern observed for mRNA (Fig. 5). Similar to the gene expression, the control samples exhibited a relatively uniform expression pattern of CDH16 across the gland, while thyroid glands exposed to 10 μM PFOS exhibited a reduced and patchy expression pattern. By staining serial sections, it was clear that the expression pattern in both control and exposed samples was largely overlapping between cadherin-16 mRNA and protein.

PFOS exposure increased expression of Tpo, Lrp2 and Pclaf in developing rat thyroid glands

Since PFOS dysregulated key components of thyroid gland development, we proceeded to investigate genes related to thyroid function. They all form part of the integrated TH biosynthesis and secretion machinery, and some are also regulated by the transcription factors (Nilsson and Fagman, 2017) (Fig. 6). PFOS significantly upregulated the expression of *Tpo* at 1 μM, and *Lrp2* at 1 and 10 μM (Fig. 6C and 6E). There were no effects on *Tshr*, *Slc5a5*(NIS), *Tg* and *Dio1* transcript levels. We also assessed the effect of PFOS on other gene transcripts of relevance to thyroid development and function (*Nectin1*, *Kcnip3*, *Wnt5b* and *Pclaf*) (Fig. S1). Here, *Pclaf* was upregulated 3-fold relative to controls (Fig. S1D) while there were no effects on expression of *Nectin1*, *Kcnip3* and *Wnt5b* (Fig. S1A-C).

We performed immunostaining of both LRP2 and PCLAF to assess protein expression. There were only minor nominal effects on the %-area positive for LRP2 and PCLAF (Fig. S2).

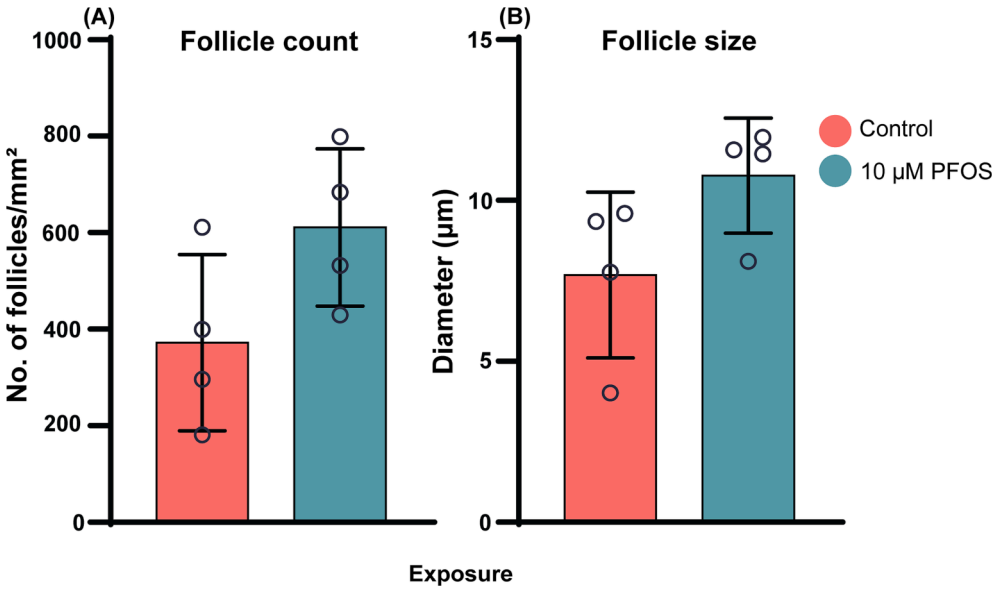

Fig. 1. The effects of PFOS on (A) Follicle count and (B) Follicle size. Thyroid glands were isolated from GD21 rat fetuses and cultured *ex vivo* with 1 µM TSH for 48 h. The glands were exposed to either 0 (Control, red) or 10 µM PFOS (green; n = 4) and the no. of follicles/mm^2 and follicle size is presented as mean ± SD, with individual data points shown as circles. No statistically significant change in the average number of follicles with lumen per mm^2 of thyroid (A), nor in the average follicle size per thyroid gland, was observed (B). PFOS: perfluorooctanesulfonic acid.

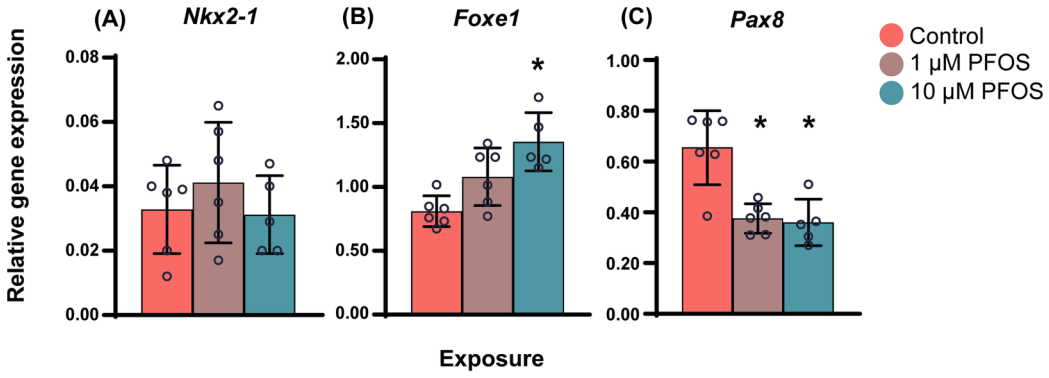

Fig. 2. Effects of PFOS on the relative transcript levels of (A) *Nkx2-1*, (B) *Foxe1*, and (C) *Pax8*. GD21 rat thyroid glands were cultured *ex vivo* with 1 µM TSH for 48 h. Thyroid glands were exposed to either 0 (Control, red), 1 (brown), or 10 µM (green) PFOS (n = 5–6). Relative gene expression was calculated using the $2^{-\Delta\Delta Ct}$ method with normalization to the geometric mean of *Rps18* and *Sdha*, and is presented as mean ± SD, with individual data points shown as circles. A significant increase in the expression of *Foxe1* was observed at 10 µM PFOS (B), while a significant downregulation was seen for *Pax8* at 1 and 10 µM (C). * $p < 0.05$, as determined by ANOVA followed by post hoc Dunnett's test. PFOS: perfluorooctanesulfonic acid.

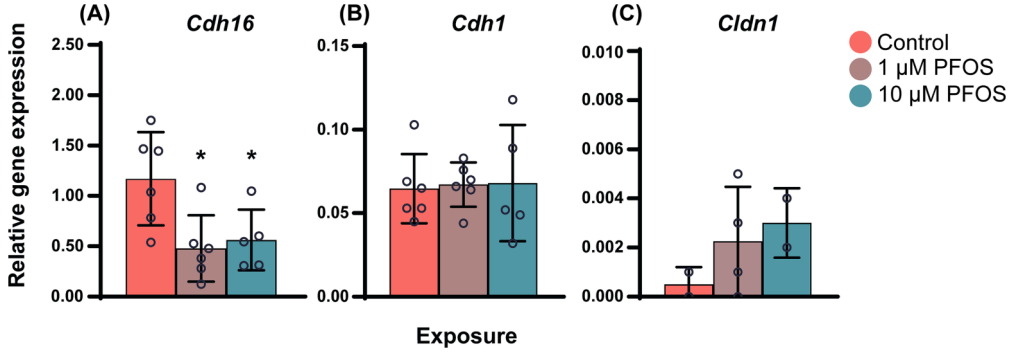

Fig. 3. Effects of PFOS on the relative transcript levels of thyroid gland transcription factor target genes (A) *Cdh16*, (B) *Cdh1*, and (C) *Cldn1*. GD21 rat thyroid glands were cultured *ex vivo* with 1 µM TSH for 48 h. Thyroid glands were exposed to either 0 (Control, red), 1 (brown), or 10 µM (green) PFOS (n = 2–6). Relative gene expression was calculated using the $2^{-\Delta\Delta Ct}$ method with normalization to the geometric mean of *Rps18* and *Sdha,* and is presented as mean ± SD, with individual data points shown as circles. Both 1 and 10 µM PFOS significantly reduced the expression of *Cdh16* (A), while *Cdh1* and *Cldn1* were not affected. * $p < 0.05$, as determined by ANOVA followed by post hoc Dunnett's test. PFOS: perfluorooctanesulfonic acid.

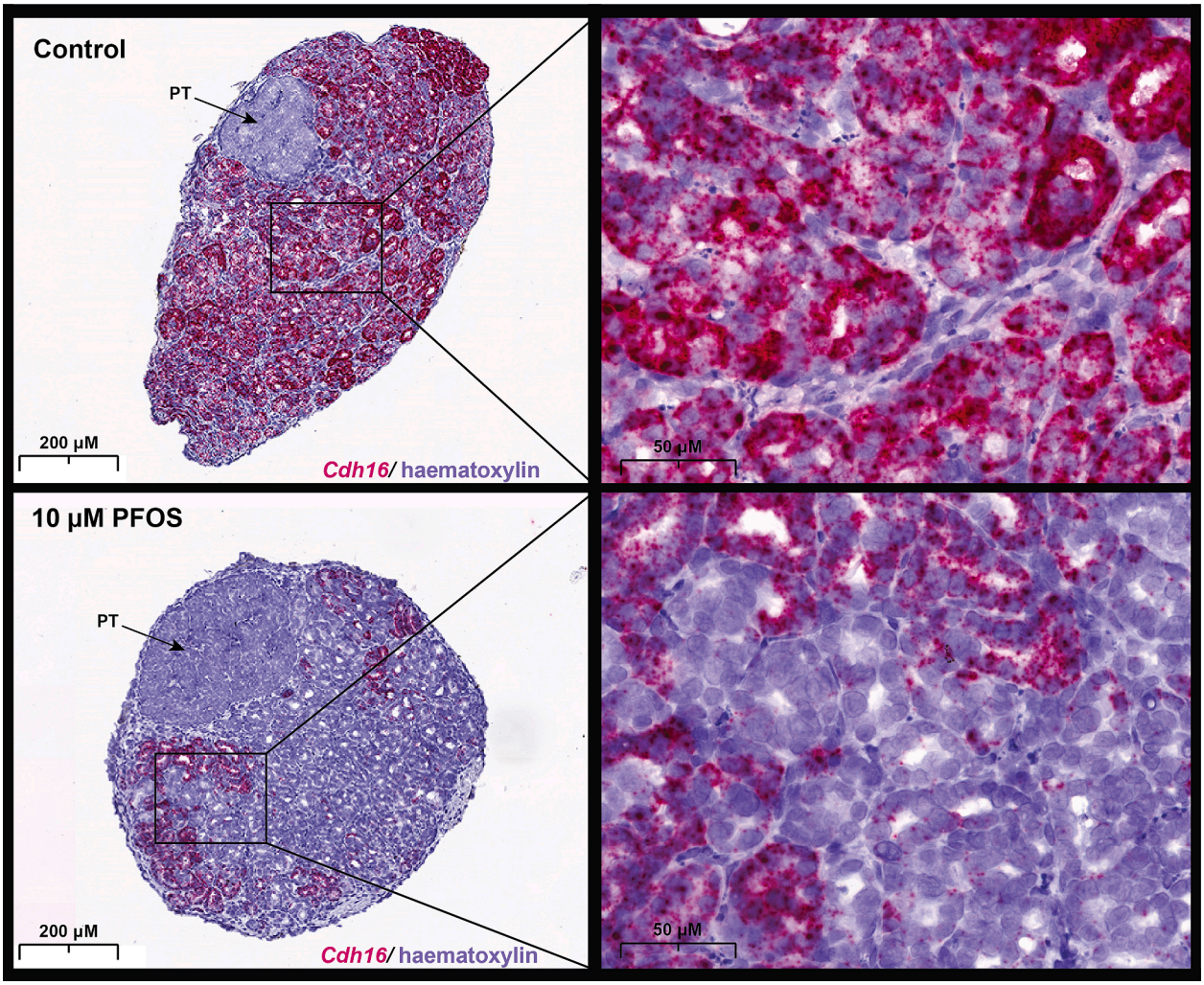

Fig. 4. PFOS exposure alters *Cdh16* expression. GD21 rat thyroid glands were cultured *ex vivo* with 1 µM TSH and either 0 (Control), or 10 µM PFOS (n = 4) for 48 h. Red staining is *Cdh16* and the purple staining is haematoxylin stained nuclei. Representative images with magnified inserts are shown. In the controls, *Cdh16* expression appeared uniform across the whole thyroid gland, except for in the parathyroid (PT). In the glands exposed to 10 µM PFOS, the expression of *Cdh16* was patchy, with some areas of high expression and others with none or very low expression. PFOS: perfluorooctanesulfonic acid; PT: parathyroid.

Discussion

The thyroid gland is vital for the health of an organism. Disrupted thyroid development or function can cause lifelong alterations in the TH system leading to chronic disease and even death (Mullur et al., 2014; Zoeller and Rovet, 2004). Congenital hypothyroidism is one of the most common neonatal birth defects, affecting 1 out of 3500 live births (Kratzsch and Pulzer, 2008) of which approximately 80 % of cases can be attributed to some form of thyroid dysgenesis (Grüters et al., 1994). This is concerning as thyroid gland development is thought to be susceptible to environmental factors (McNally et al., 2021). Adding to this, prenatal exposure to PFAS can cause lasting disruption of the TH system (Feng et al., 2017; Lau et al., 2003; Yu et al., 2009b). Here we offer a possible first step to understanding how chemicals such as PFOS can interfere with the development of the thyroid gland.

In our *ex vivo* rat culture model, PFOS exposure disrupted expression of several key transcription factors and downstream gene targets. Notably, *Foxe1* was upregulated whereas *Pax8* was downregulated in PFOS-exposed GD21 thyroid glands. These transcription factors are part of a tightly controlled network regulating thyroid gland development and function (López-Márquez et al., 2021). Disruption to this molecular machinery may thus adversely impact the formation of the thyroid gland as well as its ability to function. This could have real consequences for lifelong thyroid gland function. Although complete disruption to the transcription factor network can cause thyroid agenesis (De Felice et al., 1998; López-Márquez et al., 2021; Mansouri et al., 1998; Montanelli and Tonacchera, 2010; Nilsson and Fagman, 2017), less severe impact on the same regulatory network could potentially lead to less severe organ phenotypes. In the cultured rat thyroid glands exposed to PFOS, we did not observe marked effects on follicle counts or size after two days of culture, although there was a tendency towards increased counts. However, the calcium-dependent, membrane-associated glycoprotein CDH16 was significantly disrupted.

Cdh16 is a transcriptional target of PAX8 (de Cristofaro et al., 2012) and is thought to control the apical-basal polarization of the thyroid epithelial cells. This polarization is necessary for lumen formation, follicle growth and, ultimately, follicular function (Koumarianou et al., 2017). In the thyroid, CDH16 forms adherens junctions between the thyroid follicular epithelial cells of the follicles, which is essential for lumen formation (Koumarianou et al., 2017). The fact that PFOS exposure downregulated *Pax8* expression, as well as CDH16 expression at both transcript and protein level, may suggest that PFOS can disrupt follicle formation, maturation, and function. Since the follicles are required for TH biosynthesis (Bernier-Valentin et al., 2006; Nilsson and Fagman, 2017), this phenotype could help explain the persistent effects on TH regulation postnatally following developmental exposure to

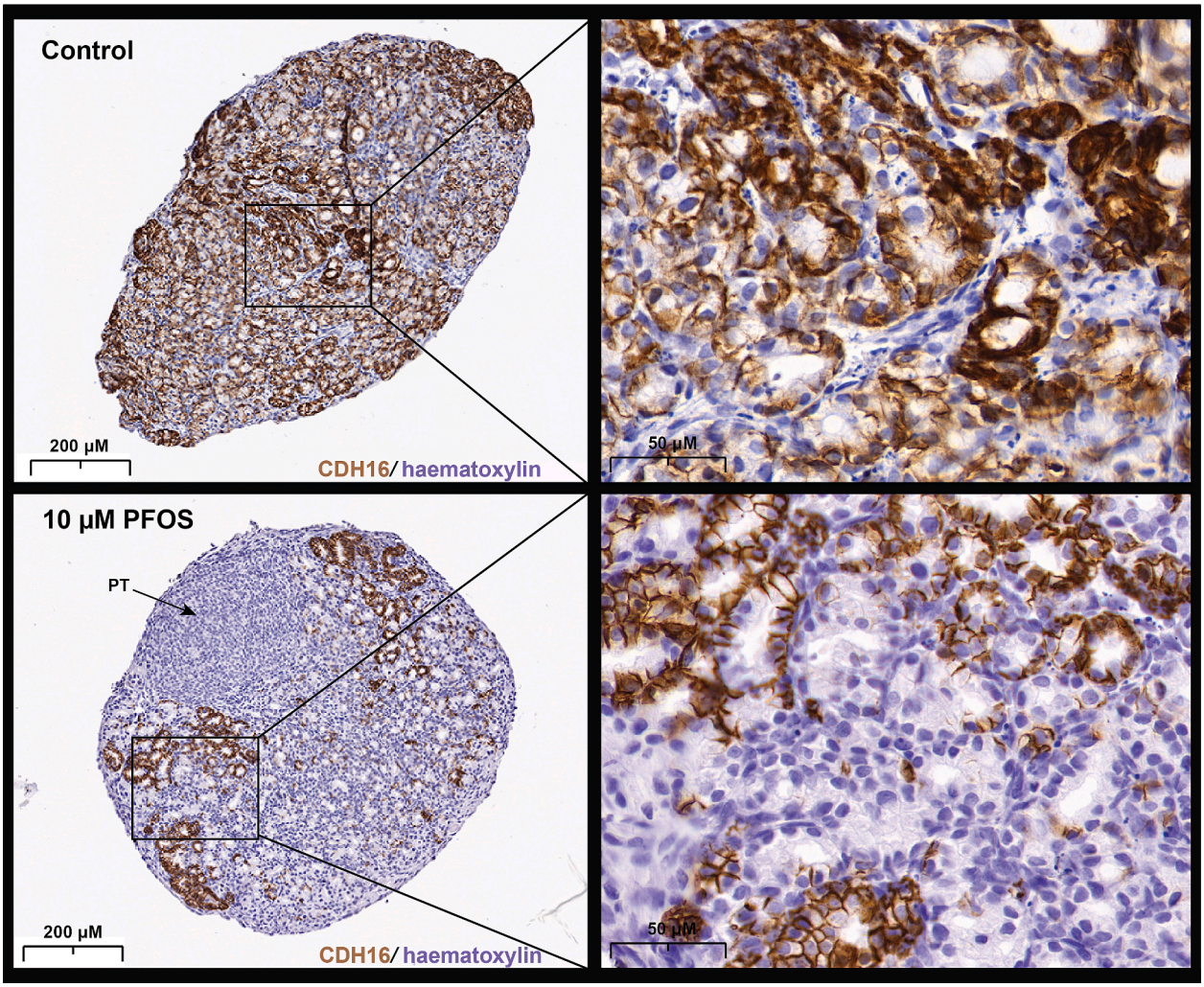

Fig. 5. PFOS exposure alters CDH16 expression. GD21 rat thyroid glands were cultured *ex vivo* with 1 µM TSH and either 0 (Control), or 10 µM PFOS (n = 4) for 48 h. In the controls, uniform expression of CDH16 can be seen versus patchy expression in the thyroid glands exposed to 10 µM PFOS. Representative images with magnified inserts are shown. Brown staining is CDH16 and purple staining is haematoxylin stained nuclei. PFOS: perfluorooctanesulfonic acid; PT: parathyroid.

PFOS, even when exposure ceases. Especially since TSH levels and TSH mediated cAMP signalling remain unaffected by PFOS (Croce et al., 2019; Lau et al., 2003; Yu et al., 2009b).

In the thyroid follicles, PFOS exposure increased expression of *Lrp2* and the FOXE1-regulated gene *Tpo* (Aza-Blanc et al., 1993; Lisi et al., 2003; Ortiga-Carvalho et al., 2016; Santisteban et al., 1992). *Lrp2* encodes for megalin, which plays a role in importing Tg from the apical surface of the follicular lumen and facilitates transport of Tg out to the blood. TPO is critical in TH synthesis where it synthetizes T3 and T4 at the interface between the apical plasma membrane and the colloid. The fact that PFOS can upregulate *Foxe1*, *Tpo* and *Lrp2* could indicate an upregulation of TH synthesis in the *ex vivo* cultured thyroid glands. In other words, the overall effect pattern observed in the *ex vivo* exposed thyroid glands could indicate that PFOS can disrupt expression of key transcription factors, ultimately disrupting TH synthesis. Alternatively, PFOS may directly disrupt follicle integrity through disruption of PAX8 and CDH16, leading to a compensatory response in the TH synthesis apparatus.

Our study provides a possible first insight into understanding the molecular underpinnings of how prenatal PFOS exposure leads to lasting decrease in TH levels in rat pups (Feng et al., 2017; Lau et al., 2003; Yu et al., 2009b), even when the body burden of PFOS decreases (Yu et al., 2009b). In zebrafish embryos, PFOS exposure can increase the expression of *Hhex* and *Pax8* (Shi et al., 2008). While in chicken embryos, exposure to a mixture of PFASs can decrease relative colloid area and thyroid follicular size, concomitant with lower free T4 and T3 levels (Mattsson et al., 2019). Although we did not observe obvious morphological differences in PFOS-exposed thyroid glands, we did observe marked changes in CDH16 expression in the follicles, which could lead to compromised tissue integrity. PFOS also increased the expression of the oncogene *Pclaf*. Since PFOS was recently classified as "possibly carcinogenic to humans" by the International Agency for Research on Cancer (IARC) (Ma et al., 2020)(Zahm et al., 2024), any potential associations between *Pclaf* and PFOS should be investigated further. Notably, our study design does have limitations, such as a limited sample size of 4 and a short exposure period of only 48 h. In addition, although thyroid glands can develop *ex vivo*, the rate at which developmental processes occur, may differ from the *in vivo* situation (Carré et al., 2020). Nevertheless, 48 h exposure did capture an acute response in both gene and protein expression.

Conclusions

PFOS-induced disturbance to thyroid gland development is of concern, as it may alter the capacity to produce THs later in life. Here we propose a possible mechanism by which PFOS can disturb the regulatory network of transcription factors guiding thyroid development and function in *ex vivo* cultured fetal rat thyroid glands. The suggested

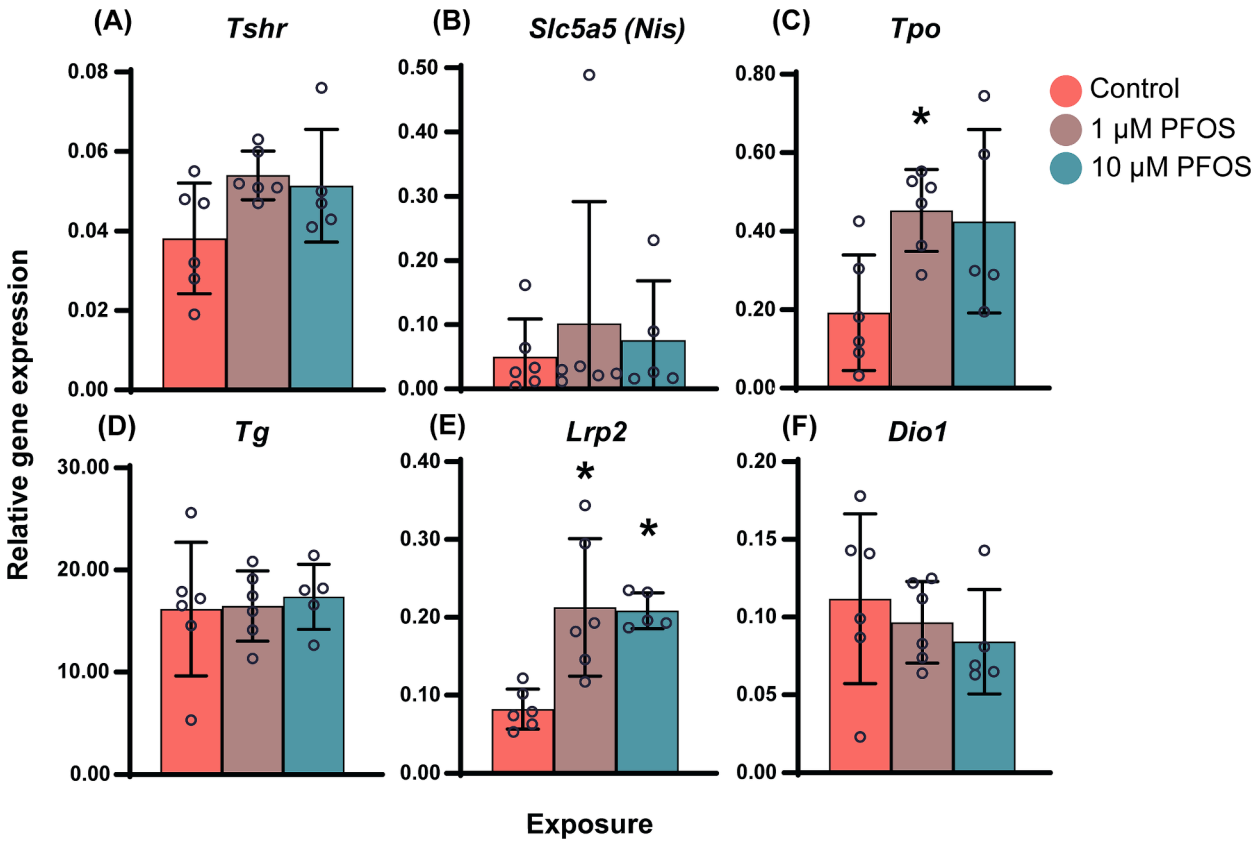

Fig. 6. Effects of PFOS on thyroid gland function and hormone synthesis gene transcripts. GD21 rat thyroid glands were cultured *ex vivo* with 1 μM TSH for 48 h. Thyroid glands were exposed to either 0 (Control, red), 1 (brown), or 10 μM (green) PFOS (n = 5–6). Gene expression was calculated using the $2^{-\Delta\Delta Ct}$ method with normalization to the geometric mean of *Rps18* and *Sdha,* and is presented as mean ± SD, with individual data points shown as circles. *Tpo* expression increased following exposure to 1 μM PFOS (C), while *Lrp2* expression increased following exposure to 1 and 10 μM PFOS (E). *Tshr* (A), *Slc5a5 (NIS)* (B), *Tg* (D), *Dio1* (F) were not affected. (A-D) and (F): * $p < 0.05$, as determined by ANOVA followed by post hoc Dunnett's test. (E): Assumptions for ANOVA were not met, * $p < 0.05$, as determined by Kruskal-Wallis followed by post hoc Dunn's test. PFOS: perfluorooctanesulfonic acid.

mechanism implies that PFOS can affect thyroid development and function through increased expression of *Foxe1* and reduced expression of *Pax8* and *Cdh16*/CDH16. Additionally, our data indicate that PFOS can upregulate the TH synthesis genes *Tpo* and *Lrp2*, possibly as a compensatory effect on TH synthesis. Disruption to these processes may adversely affect the function of the TH system both during gestation and later in life. Further studies are needed to establish whether these effects are a driving factor in PFOS-induced TH system disruption and whether similar effects occur *in vivo*.

Funding

This project was funded by the Ministry of Foods, Agriculture and Fisheries of Denmark (FEMINIX project). The funding source was not involved in the study design, data collection and analysis, or report preparation.

CRediT authorship contribution statement

Nichlas Davidsen: Conceptualization, Methodology, Formal analysis, Investigation, Writing – original draft, Writing – review & editing, Visualization, Project administration. **Louise Ramhøj:** Conceptualization, Methodology, Formal analysis, Investigation, Writing – original draft, Writing – review & editing, Visualization, Project administration. **Anne-Sofie Ravn Ballegaard:** Formal analysis, Investigation, Writing – review & editing. **Anna Kjerstine Rosenmai:** Methodology, Writing – review & wditing, Project administration. **Cecillie Sofie Henriksen:** Formal analysis, Investigation, Writing – review & editing. **Terje Svingen:** Conceptualization, Investigation, Resources, Writing – original draft, Writing – review & editing, Visualization, Project administration, Funding acquisition.

Declaration of competing interest

The authors declare that they have no known competing financial interests or personal relationships that could have appeared to influence the work reported in this paper.

Data availability

Data will be made available on request.

Acknowledgements

We would like to thank our technicians Lillian Sztuk, Dorte Lykkegaard Korsbech and Mette Voigt Jessen for their valuable contributions. Histology data were generated through accessing research infrastructure at DTU National Food Institute, including FOODHAY equipment (Food and Health Open Innovation Laboratory, Danish Roadmap for Research Infrastructure).

Appendix A. Supplementary data

Supplementary data to this article can be found online at https://doi.org/10.1016/j.crtox.2024.100154.

References

Aimuzi, R., Luo, K., Chen, Q., Wang, H., Feng, L., Ouyang, F., Zhang, J., 2019. Perfluoroalkyl and polyfluoroalkyl substances and fetal thyroid hormone levels in umbilical cord blood among newborns by prelabor cesarean delivery. Environ. Int. 130, 104929 https://doi.org/10.1016/J.ENVINT.2019.104929.

Aza-Blanc, P., Di Lauro, R., Santisteban, P., 1993. Identification of a cis-regulatory element and a thyroid-specific nuclear factor mediating the hormonal regulation of rat thyroid peroxidase promoter activity. Mol. Endocrinol. 7, 1297–1306. https://doi.org/10.1210/MEND.7.10.8264661.

Bernier-Valentin, F., Trouttet-Masson, S., Rabilloud, R., Selmi-Ruby, S., Rousset, B., 2006. Three-dimensional organization of thyroid cells into follicle structures is a pivotal factor in the control of sodium/iodide symporter expression. Endocrinology 147, 2035–2042. https://doi.org/10.1210/EN.2005-0805.

Buckalew, A.R., Wang, J., Murr, A.S., Deisenroth, C., Stewart, W.M., Stoker, T.E., Laws, S.C., 2020. Evaluation of potential sodium-iodide symporter (NIS) inhibitorsusing a secondary Fischer rat thyroid follicular cell (FRTL-5) radioactiveiodide uptake (RAIU) assay. Arch. Toxicol. 94, 873. https://doi.org/10.1007/S00204-020-02664-Y.

Carré, A., Gawade, S., Dertschnig, S., Hafen, K., Polak, M., Szinnai, G., 2020. Ex vivo model for elucidating the functional and structural differentiation of the embryonic mouse thyroid. Mol. Cell. Endocrinol. 510, 110834 https://doi.org/10.1016/J.MCE.2020.110834.

Chang, S.C., Thibodeaux, J.R., Eastvold, M.L., Ehresman, D.J., Bjork, J.A., Froehlich, J. W., Lau, C., Singh, R.J., Wallace, K.B., Butenhoff, J.L., 2008. Thyroid hormone status and pituitary function in adult rats given oral doses of perfluorooctanesulfonate (PFOS). Toxicology 243, 330–339. https://doi.org/10.1016/J.TOX.2007.10.014.

Conti, A., Strazzeri, C., Rhoden, K.J., 2020. Perfluorooctane sulfonic acid, a persistent organic pollutant, inhibits iodide accumulation by thyroid follicular cells in vitro. Mol. Cell. Endocrinol. 515, 110922 https://doi.org/10.1016/J.MCE.2020.110922.

Coperchini, F., Pignatti, P., Lacerenza, S., Negri, S., Sideri, R., Testoni, C., de Martinis, L., Cottica, D., Magri, F., Imbriani, M., Rotondi, M., Chiovato, L., 2014. Exposure to perfluorinated compounds: in vitro study on thyroid cells. Environ. Sci. Pollut. Res. 2014 223 22, 2287–2294. https://doi.org/10.1007/S11356-014-3480-9.

Croce, L., Coperchini, F., Tonacchera, M., Imbriani, M., Rotondi, M., Chiovato, L., 2019. Effect of long- and short-chain perfluorinated compounds on cultured thyroid cells viability and response to TSH. J. Endocrinol. Invest. 42, 1329–1335. https://doi.org/10.1007/S40618-019-01062-1/METRICS.

Curran, I., Hierlihy, S.L., Liston, V., Pantazopoulos, P., Nunnikhoven, A., Tittlemier, S., Barker, M., Trick, K., Bondy, G., 2008. Altered fatty acid homeostasis and related toxicologic sequelae in rats exposed to dietary potassium perfluorooctanesulfonate (PFOS). J. Toxicol. Environ. Heal. Part A 71, 1526–1541. https://doi.org/10.1080/15287390802361763.

Damante, G., Tell, G., Di Lauro, R., 2000. A unique combination of transcription factors controls differentiation of thyroid cells. Prog. Nucleic Acid Res. Mol. Biol. 66, 307–356. https://doi.org/10.1016/S0079-6603(00)66033-6.

Davidsen, N., Ramhøj, L., Lykkebo, C.A., Kugathas, I., Poulsen, R., Rosenmai, A.K., Evrard, B., Darde, T.A., Axelstad, M., Bahl, M.I., Hansen, M., Chalmel, F., Licht, T.R., Svingen, T., 2022. PFOS-induced thyroid hormone system disrupted rats display organ-specific changes in their transcriptomes. Environ. Pollut. 305, 119340 https://doi.org/10.1016/J.ENVPOL.2022.119340.

de Cristofaro, T., di Palma, T., Fichera, I., Lucci, V., Parrillo, L., de Felice, M., Zannini, M., 2012. An essential role for Pax8 in the transcriptional regulation of cadherin-16 in thyroid cells. Mol. Endocrinol. 26, 67. https://doi.org/10.1210/ME.2011-1090.

De Escobar, G.M., Obregón, M.J., Del Rey, F.E., 2004. Role of thyroid hormone during early brain development. Eur. J. Endocrinol. 151, U25–U37. https://doi.org/10.1530/EJE.0.151U025.

De Felice, M., Ovitt, C., Biffali, E., Rodriguez-Mallon, A., Arra, C., Anastassiadis, K., Macchia, P.E., Mattei, M.G., Mariano, A., Schöler, H., Macchia, V., Di Lauro, R., 1998. A mouse model for hereditary thyroid dysgenesis and cleft palate. Nat. Genet. 1998 194 19, 395–398. https://doi.org/10.1038/1289.

Feng, X., Cao, X., Zhao, S., Wang, X., Hua, X., Chen, L., Chen, L., 2017. Exposure of Pregnant Mice to Perfluorobutanesulfonate Causes Hypothyroxinemia and Developmental Abnormalities in Female Offspring. Toxicol. Sci. 155, 409–419. https://doi.org/10.1093/TOXSCI/KFW219.

Fenton, S.E., Ducatman, A., Boobis, A., DeWitt, J.C., Lau, C., Ng, C., Smith, J.S., Roberts, S.M., 2021. Per- and Polyfluoroalkyl Substance Toxicity and Human Health Review: Current State of Knowledge and Strategies for Informing Future Research. Environ. Toxicol. Chem. 40, 606. https://doi.org/10.1002/ETC.4890.

Gilbert, M.E., O'Shaughnessy, K.L., Thomas, S.E., Riutta, C., Wood, C.R., Smith, A., Oshiro, W.O., Ford, R.L., Hotchkiss, M.G., Hassan, I., Ford, J.L., 2021. Thyroid Disruptors: Extrathyroidal Sites of Chemical Action and Neurodevelopmental Outcome—An Examination Using Triclosan and Perfluorohexane Sulfonate. Toxicol. Sci. 183, 195–213. https://doi.org/10.1093/TOXSCI/KFAB080.

Grüters, A., Finke, R., Krude, H., Meinhold, H., 1994. Etiological Grouping of Permanent Congenital Hypothyroidism with a Thyroid Gland in situ. Horm. Res. 41, 3–9. https://doi.org/10.1159/000183869.

Johansson, E., Liang, S., Moccia, C., Carlsson, T., Andersson, D., Fagman, H., Nilsson, M., 2021. Asynchrony of Apical Polarization, Luminogenesis, and Functional Differentiation in the Developing Thyroid Gland. Front. Endocrinol. (Lausanne) 12, 760541. https://doi.org/10.3389/FENDO.2021.760541/BIBTEX.

Koumarianou, P., Goméz-López, G., Santisteban, P., Ewald, A., 2017. Pax8 controls thyroid follicular polarity through cadherin-16. J. Cell Sci. 130, 219–231. https://doi.org/10.1242/JCS.184291.

Kratzsch, J., Pulzer, F., 2008. Thyroid gland development and defects. Best Pract. Res. Clin. Endocrinol. Metab. 22, 57–75. https://doi.org/10.1016/J.BEEM.2007.08.006.

Lau, C., Thibodeaux, J.R., Hanson, R.G., Rogers, J.M., Grey, B.E., Stanton, M.E., Buttenhoff, J.L., Stevenson, L.A., 2003. Exposure to perfluorooctane sulfonate during pregnancy in rat and mouse. II: Postnatal evaluation. Toxicol. Sci. https://doi.org/10.1093/toxsci/kfg122.

Lisi, S., Pinchera, A., McCluskey, R.T., Willnow, T.E., Refetoff, S., Marcocci, C., Vitti, P., Menconi, F., Grasso, L., Luchetti, F., Collins, A.B., Marinò, M., 2003. Preferential megalin-mediated transcytosis of low-hormonogenic thyroglobulin: A control mechanism for thyroid hormone release. Proc. Natl. Acad. Sci. USA 100, 14858–14863. https://doi.org/10.1073/PNAS.2432267100/ASSET/B28D0332-58CD-452A-8804-E3AD11E68A42/ASSETS/GRAPHIC/PQ2432267007.JPEG.

López-Márquez, A., Carrasco-López, C., Fernández-Méndez, C., Santisteban, P., 2021. Unraveling the Complex Interplay Between Transcription Factors and Signaling Molecules in Thyroid Differentiation and Function, From Embryos to Adults. Front. Endocrinol. (Lausanne) 12, 1. https://doi.org/10.3389/FENDO.2021.654569.

Ma, F.F., Zhi, C., Wang, M., Li, T., Khan, S.A., Ma, Z., Jing, Z., Bo, C., Zhou, Q., Xia, S., Huang, S., Huang, S., Zhang, Z., Jia, H., Cui, X., Yao, M., Ji, T., 2020. Dysregulated NF-κB signal promotes the hub gene PCLAF expression to facilitate nasopharyngeal carcinoma proliferation and metastasis. Biomed. Pharmacother. 125, 109905 https://doi.org/10.1016/J.BIOPHA.2020.109905.

Maenhaut, C., Brabant, G., Vassart, G., Dumont, J.E., 1992. In vitro and in vivo regulation of thyrotropin receptor mRNA levels in dog and human thyroid cells. J. Biol. Chem. 267, 3000–3007. https://doi.org/10.1016/S0021-9258(19)50686-X.

Mansouri, A., Chowdhury, K., Gruss, P., 1998. Follicular cells of the thyroid gland require Pax8 gene function. Nat. Genet. 1998 191 19, 87–90. https://doi.org/10.1038/ng0598-87.

Mattsson, A., Sjöberg, S., Kärrman, A., Brunström, B., 2019. Developmental exposure to a mixture of perfluoroalkyl acids (PFAAs) affects the thyroid hormone system and the bursa of Fabricius in the chicken. Sci. Reports 2019 91 9, 1–14. https://doi.org/10.1038/s41598-019-56200-9.

McNally, R.J.Q., Jones, J.H., Shaikh, M.G., Donaldson, M.D.C., Blakey, K., Cheetham, T. D., 2021. Congenital Hypothyroidism: Space-Time Clustering of Thyroid Dysgenesis Indicates a Role for Environmental Factors in Disease Etiology. Thyroid 31, 876–883. https://doi.org/10.1089/thy.2020.0005.

Montanelli, L., Tonacchera, M., 2010. Genetics and phenomics of hypothyroidism and thyroid dys- and agenesis due to PAX8 and TTF1 mutations. Mol. Cell. Endocrinol. 322, 64–71. https://doi.org/10.1016/J.MCE.2010.03.009.

Mullur, R., Liu, Y.-Y., Brent, G.A., 2014. Thyroid Hormone Regulation of Metabolism. Physiol. Rev. 94, 355. https://doi.org/10.1152/PHYSREV.00030.2013.

Nilsson, M., Fagman, H., 2017. Development of the Thyroid Gland. Development 144, 2123–2140. https://doi.org/10.1242/DEV.145615.

Ortiga-Carvalho, T.M., Chiamolera, M.I., Pazos-Moura, C.C., Wondisford, F.E., 2016. Hypothalamus-Pituitary-Thyroid Axis. Compr. Physiol. 6, 1387–1428. https://doi.org/10.1002/CPHY.C150027.

Parlato, R., Rosica, A., Rodriguez-Mallon, A., Affuso, A., Postiglione, M.P., Arra, C., Mansouri, A., Kimura, S., Di Lauro, R., De Felice, M., 2004. An integrated regulatory network controlling survival and migration in thyroid organogenesis. Dev. Biol. 276, 464–475. https://doi.org/10.1016/J.YDBIO.2004.08.048.

Pirali, B., Negri, S., Chytiris, S., Perissi, A., Villani, L., La Manna, L., Cottica, D., Ferrari, M., Imbriani, M., Rotondi, M., Chiovato, L., 2009. Perfluorooctane sulfonate and perfluorooctanoic acid in surgical thyroid specimens of patients with thyroid diseases. Thyroid 19, 1407–1412. https://doi.org/10.1089/thy.2009.0174.

Postiglione, M.P., Parlato, R., Rodriguez-Mallon, A., Rosica, A., Mithbaokar, P., Maresca, M., Marians, R.C., Davies, T.F., Zannini, M.S., Felice, M.D., Lauro, R.D., 2002. Role of the thyroid-stimulating hormone receptor signaling in development and differentiation of the thyroid gland. Proc. Natl. Acad. Sci. 99, 15462–15467. https://doi.org/10.1073/PNAS.242328999.

Preston, E.V., Webster, T.F., Claus Henn, B., McClean, M.D., Gennings, C., Oken, E., Rifas-Shiman, S.L., Pearce, E.N., Calafat, A.M., Fleisch, A.F., Sagiv, S.K., 2020. Prenatal Exposure to Per- and Polyfluoroalkyl Substances and Maternal and Neonatal Thyroid Function in the Project Viva Cohort: a mixtures approach. Environ. Int. 139, 105728 https://doi.org/10.1016/J.ENVINT.2020.105728.

Ramhøj, L., Svingen, T., Frädrich, C., Rijntjes, E., Wirth, E.K., Pedersen, K., Köhrle, J., Axelstad, M., 2022. Perinatal exposure to the thyroperoxidase inhibitors methimazole and amitrole perturbs thyroid hormone system signaling and alters motor activity in rat offspring. Toxicol. Lett. 354, 44–55. https://doi.org/10.1016/J.TOXLET.2021.10.010.

Ren, X.M., Zhang, Y.F., Guo, L.H., Qin, Z.F., Lv, Q.Y., Zhang, L.Y., 2014. Structure–activity relations in binding of perfluoroalkyl compounds to human thyroid hormone T3 receptor. Arch. Toxicol. 2014 892 89, 233–242. https://doi.org/10.1007/S00204-014-1258-Y.

Ren, X.M., Qin, W.P., Cao, L.Y., Zhang, J., Yang, Y., Wan, B., Guo, L.H., 2016. Binding interactions of perfluoroalkyl substances with thyroid hormone transport proteins and potential toxicological implications. Toxicology 366–367, 32–42. https://doi.org/10.1016/J.TOX.2016.08.011.

Santisteban, P., Acebrón, A., Polycarpou-Schwarz, M., Di Lauro, R., 1992. Insulin and insulin-like growth factor I regulate a thyroid-specific nuclear protein that binds to the thyroglobulin promoter. Mol. Endocrinol. 6, 1310–1317. https://doi.org/10.1210/MEND.6.8.1406708.

Schindelin, J., Arganda-Carreras, I., Frise, E., Kaynig, V., Longair, M., Pietzsch, T., Preibisch, S., Rueden, C., Saalfeld, S., Schmid, B., Tinevez, J.Y., White, D.J., Hartenstein, V., Eliceiri, K., Tomancak, P., Cardona, A., 2012. Fiji: an open-source platform for biological-image analysis. Nat. Methods 2012 97 9, 676–682. https://doi.org/10.1038/nmeth.2019.

Schmittgen, T.D., Livak, K.J., 2008. Analyzing real-time PCR data by the comparative CT method. Nat. Protoc. 2008 36 3, 1101–1108. https://doi.org/10.1038/nprot.2008.73.

Shi, X., Du, Y., Lam, P.K.S., Wu, R.S.S., Zhou, B., 2008. Developmental toxicity and alteration of gene expression in zebrafish embryos exposed to PFOS. Toxicol. Appl. Pharmacol. 230, 23–32. https://doi.org/10.1016/J.TAAP.2008.01.043.

Thibodeaux, J.R., Hanson, R.G., Rogers, J.M., Grey, B.E., Barbee, B.D., Richards, J.H., Butenhoff, J.L., Stevenson, L.A., Lau, C., 2003. Exposure to Perfluorooctane Sulfonate during Pregnancy in Rat and Mouse. I: Maternal and Prenatal Evaluations. Toxicol. Sci. 74, 369–381. https://doi.org/10.1093/TOXSCI/KFG121.

Wang, F., Flanagan, J., Su, N., Wang, L.C., Bui, S., Nielson, A., Wu, X., Vo, H.T., Ma, X.J., Luo, Y., 2012. RNAscope: A Novel in Situ RNA Analysis Platform for Formalin-Fixed. Paraffin-Embedded Tissues. J. Mol. Diagn. 14, 22. https://doi.org/10.1016/J.JMOLDX.2011.08.002.

Wang, J., Hallinger, D.R., Murr, A.S., Buckalew, A.R., Simmons, S.O., Laws, S.C., Stoker, T.E., 2018. High-Throughput Screening and Quantitative Chemical Ranking for Sodium-Iodide Symporter Inhibitors in ToxCast Phase I Chemical Library. Environ. Sci. Technol. 52, 5417–5426. https://doi.org/10.1021/acs.est.7b06145.

Wang, J., Hallinger, D.R., Murr, A.S., Buckalew, A.R., Lougee, R.R., Richard, A.M., Laws, S.C., Stoker, T.E., 2019. High-throughput screening and chemotype-enrichment analysis of ToxCast phase II chemicals evaluated for human sodium-iodide symporter (NIS) inhibition. Environ. Int. 126, 377. https://doi.org/10.1016/J.ENVINT.2019.02.024.

Weiss, J.M., Andersson, P.L., Lamoree, M.H., Leonards, P.E.G., Van Leeuwen, S.P.J., Hamers, T., 2009. Competitive Binding of Poly- and Perfluorinated Compounds to the Thyroid Hormone Transport Protein Transthyretin. Toxicol. Sci. 109, 206–216. https://doi.org/10.1093/TOXSCI/KFP055.

Yu, W.G., Liu, W., Jin, Y.H., 2009a. Effects of perfluorooctane sulfonate on rat thyroid hormone biosynthesis and metabolism. Environ. Toxicol. Chem. 28, 990–996. https://doi.org/10.1897/08-345.1.

Yu, W.G., Liu, W., Jin, Y.H., Liu, X.H., Wang, F.Q., Liu, L., Nakayama, S.F., 2009b. Prenatal and Postnatal Impact of Perfluorooctane Sulfonate (PFOS) on Rat Development: A Cross-Foster Study on Chemical Burden and Thyroid Hormone System. Environ. Sci. Technol. 43, 8416–8422. https://doi.org/10.1021/ES901602D.

Yu, W.G., Liu, W., Liu, L., Jin, Y.H., 2011. Perfluorooctane sulfonate increased hepatic expression of OAPT2 and MRP2 in rats. Arch. Toxicol. 85, 613–621. https://doi.org/10.1007/s00204-010-0613-x.

Zahm, S., Bonde, J.P., Chiu, W.A., Hoppin, J., Kanno, J., Abdallah, M., Blystone, C.R., Calkins, M.M., Dong, G.-H., Dorman, D.C., Fry, R., Guo, H., Haug, L.S., Hofmann, J. N., Iwasaki, M., Machala, M., Mancini, F.R., Maria-Engler, S.S., Møller, P., Ng, J.C., Pallardy, M., Post, G.B., Salihovic, S., Schlezinger, J., Soshilov, A., Steenland, K., Steffensen, I.-L., Tryndyak, V., White, A., Woskie, S., Fletcher, T., Ahmadi, A., Ahmadi, N., Benbrahim-Tallaa, L., Bijoux, W., Chittiboyina, S., de Conti, A., Facchin, C., Madia, F., Mattock, H., Merdas, M., Pasqual, E., Suonio, E., Viegas, S., Zupunski, L., Wedekind, R., Schubauer-Berigan, M.K., 2024. Carcinogenicity of perfluorooctanoic acid and perfluorooctanesulfonic acid. Lancet Oncol. 25, 16–17. https://doi.org/10.1016/S1470-2045(23)00622-8.

Zoeller, R.T., Rovet, J., 2004. Timing of Thyroid Hormone Action in the Developing Brain: Clinical Observations and Experimental Findings. J. Neuroendocrinol. 16, 809–818. https://doi.org/10.1111/J.1365-2826.2004.01243.X.